Nitric Oxide Is Involved in Cadmium-Induced Programmed Cell Death in Arabidopsis Suspension Cultures[1][C][W]

Roberto De Michele*, Emanuela Vurro, Chiara Rigo, Alex Costa, Lisa Elviri, Marilena Di Valentin, Maria Careri, Michela Zottini, Luigi Sanità di Toppi, and Fiorella Lo Schiavo

Dipartimento di Biologia, Università degli Studi di Padova, I–35131 Padova, Italy (R.D.M., C.R., A.C., M.Z., F.L.S.); Dipartimento di Biologia Evolutiva e Funzionale, Università degli Studi di Parma, I–43100 Parma, Italy (E.V., L.S.d.T.); Dipartimento di Chimica Generale ed Inorganica, Chimica Analitica, Chimica Fisica, Università degli Studi di Parma, I–43100 Parma, Italy (L.E., M.C.); and Dipartimento di Scienze Chimiche, Università degli Studi di Padova, I–35131 Padova, Italy (M.D.V.)

Exposure to cadmium (Cd^{2+}) can result in cell death, but the molecular mechanisms of Cd^{2+} cytotoxicity in plants are not fully understood. Here, we show that Arabidopsis (*Arabidopsis thaliana*) cell suspension cultures underwent a process of programmed cell death when exposed to 100 and 150 μM $CdCl_2$ and that this process resembled an accelerated senescence, as suggested by the expression of the marker *senescence-associated gene12* (*SAG12*). $CdCl_2$ treatment was accompanied by a rapid increase in nitric oxide (NO) and phytochelatin synthesis, which continued to be high as long as cells remained viable. Hydrogen peroxide production was a later event and preceded the rise of cell death by about 24 h. Inhibition of NO synthesis by N^G-monomethyl-arginine monoacetate resulted in partial prevention of hydrogen peroxide increase, *SAG12* expression, and mortality, indicating that NO is actually required for Cd^{2+}-induced cell death. NO also modulated the extent of phytochelatin content, and possibly their function, by *S*-nitrosylation. These results shed light on the signaling events controlling Cd^{2+} cytotoxicity in plants.

Cadmium (Cd^{2+}) is a heavy metal with a long biological half-life, and its presence as a pollutant in agricultural soil is due mainly to anthropogenic activities. It is rapidly taken up by roots and enters the food chain, resulting in toxicity for both plants and animals (for review, see Sanità di Toppi and Gabbrielli, 1999). Cd^{2+} inhibits seed germination, decreases plant growth and photosynthesis, and impairs the distribution of nutrients. Overall, the symptoms of chronic exposure to sublethal amounts of Cd^{2+} mimic premature senescence (Rascio et al., 1993; McCarthy et al., 2001; Sandalio et al., 2001; Rodriguez-Serrano et al., 2006). Depending on the concentration, Cd^{2+} treatment of tobacco (*Nicotiana tabacum*) cell cultures and onion (*Allium cepa*) roots eventually triggers either necrosis or programmed cell death (PCD; Fojtovà and Kovařik, 2000; Behboodi and Samadi, 2004).

Although Cd^{2+} is an environmental threat, the mechanisms by which it exerts its toxic effects in plants are not fully understood. In plant cells, Cd^{2+} is believed to enter through Fe^{2+}, Ca^{2+}, and Zn^{2+} transporters/channels (Clemens, 2006). Once in the cytosol, Cd^{2+} stimulates the production of phytochelatins (PCs), a glutathione-derived class of peptides containing repeated units of Glu and Cys, which bind the metal ions and transport them into the vacuole (Sanità di Toppi and Gabbrielli, 1999). Strong evidence exists that high (millimolar) concentrations of Cd^{2+} induce reactive oxygen species (ROS) bursts in plants, which might have a role in signaling and/or degenerative steps leading to cell death (Piqueras et al., 1999; Olmos et al., 2003; Cho and Seo, 2005; Garnier et al., 2006). Treatment with a lower, nontoxic Cd^{2+} concentration also caused increase in ROS production in pea (*Pisum sativum*) leaves and roots (Sandalio et al., 2001; Romero-Puertas et al., 2004; Rodriguez-Serrano et al., 2006) and Arabidopsis (*Arabidopsis thaliana*) cell cultures (Horemans et al., 2007).

Nitric oxide (NO) is a gaseous reactive molecule with a pivotal signaling role in many developmental and response processes (for review, see Neill et al., 2003; Besson-Bard et al., 2008). In plants, it can be synthesized via several routes, either enzymatically or by chemical reduction of nitrite. Nitrate reductase and a root-specific plasma membrane nitrite-NO reductase also utilize nitrite as substrate. In animals, nitric oxide synthase (NOS) converts L-Arg into NO and L-citrulline.

[1] This work was supported by the Ministero dell'Istruzione, dell'Università e della Ricerca (grant no. PRIN 2006 to F.L.S.).

* Corresponding author; e-mail demicheler@virgilio.it.

The author responsible for distribution of materials integral to the findings presented in this article in accordance with the policy described in the Instructions for Authors (www.plantphysiol.org) is: Roberto De Michele (demicheler@virgilio.it).

[C] Some figures in this article are displayed in color online but in black and white in the print edition.

[W] The online version of this article contains Web-only data.

www.plantphysiol.org/cgi/doi/10.1104/pp.108.133397

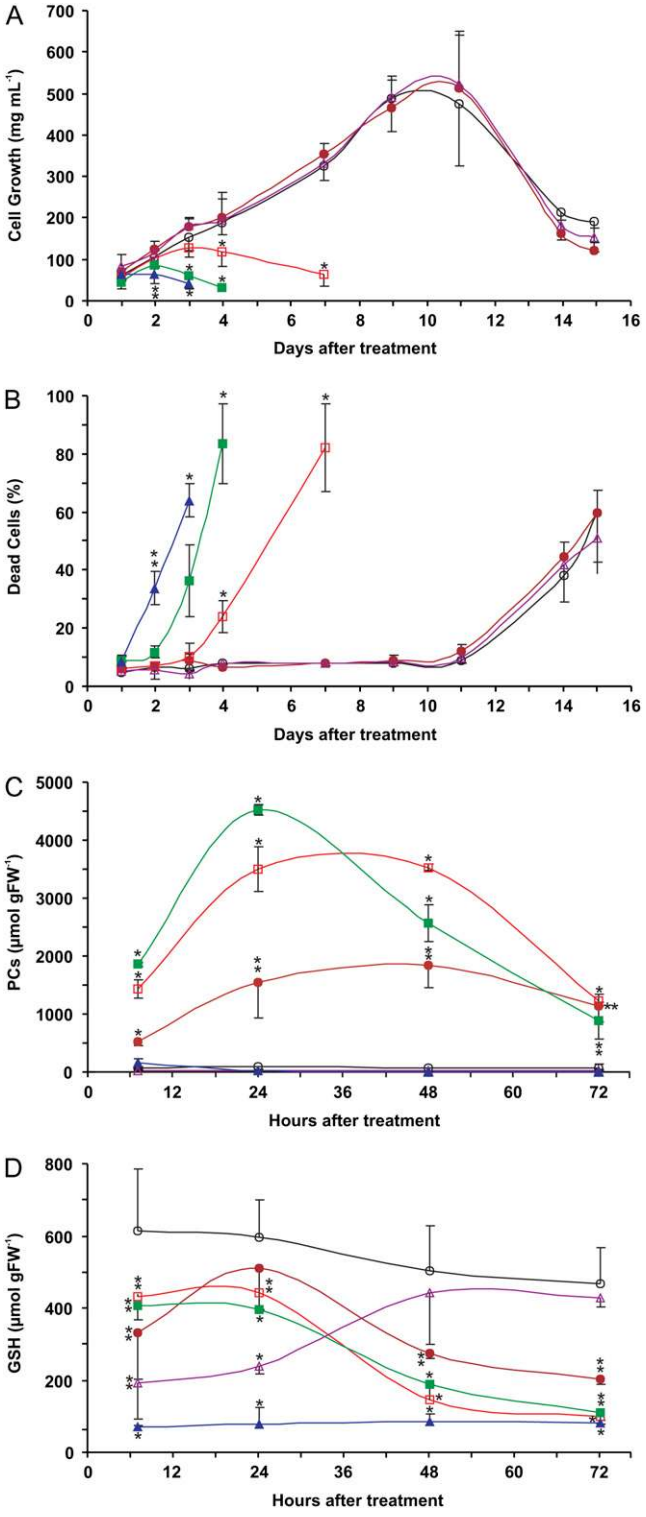

Figure 1. Events following $CdCl_2$ treatment. Three-day-old Arabidopsis cells were treated with 50, 100, or 150 μM $CdCl_2$. Pretreatment with BSO was performed when appropriate. Open circles, Control; closed circles, 50 μM $CdCl_2$; open squares, 100 μM $CdCl_2$; closed squares, 150 μM $CdCl_2$; open triangles, BSO; closed triangles, 50 μM $CdCl_2$ + BSO. A, Fresh weight (mg mL^{-1}) of cells at different times after treatment. B, Cell viability (Evans blue staining). C, Total PC content, measured as μmol sulfhydryls per gram fresh weight. D, GSH content, measured as μmol per gram fresh weight. Asterisks indicate values that are significantly different from those of untreated cells by Student's *t* test (* $P < 0.01$, ** $P < 0.05$). FW, Fresh weight. [See online article for color version of this figure.]

Although no plant NOS has been unambiguously identified yet, activity assays and pharmacological evidence suggests the existence of a NOS-like counterpart in plants. Depending on its concentration and possibly on the timing and localization of its production, NO can either act as an antioxidant or promote PCD, often in concert with ROS (Delledonne et al., 2001; Beligni et al., 2002; de Pinto et al., 2006). Extensive research has shown that NO plays a fundamental role in the hypersensitive response, but its involvement in other types of PCD, such as that resulting from mechanical stress and natural and cytokinin-induced senescence of cell cultures, has also been demonstrated (Garcês et al., 2001; Carimi et al., 2005). Because of its participation in numerous biotic and abiotic responses, NO has been proposed as a general stress molecule (Gould et al., 2003). However, the mechanisms by which NO determines its effects are far from being completely elucidated, and a number of downstream signaling pathways, involving Ca^{2+}, cyclic GMP, and cyclic ADP-Rib, are involved (Neill et al., 2003; Besson-Bard et al., 2008). NO can also modulate biological responses by direct modification of proteins, reacting with Cys residues (*S*-nitrosylation), Tyr residues (nitration), or iron and zinc in metalloproteins (metal nitrosylation; Besson-Bard et al., 2008).

The aim of this work is to study the plant responses to various concentrations of Cd^{2+} and, in particular, the role of ROS and NO in the signaling events leading to cell death. Cell cultures of the model plant Arabidopsis were chosen as an experimental system because the homogeneity and undifferentiated state of the cells, combined with the uniform delivery of the treatments, allow a clear and reproducible response. The results point to NO as a master regulator of Cd^{2+}-induced cell death. Possible mechanisms that explain this evidence will be discussed.

RESULTS

Phytochelatins Enhance Tolerance to Cd^{2+}

Arabidopsis cell suspension cultures were treated with 50, 100, and 150 μM $CdCl_2$, and their growth and viability were measured at different times after treatment. The fresh weight of cells grown with 50 μM $CdCl_2$ did not differ from that of untreated cells at any time during analysis. Their mass increased until 9 to 11 d after treatment, and later, cells underwent a senescence phase characterized by a gradual rise in cell death (Fig. 1, A and B). On the other hand, treatments with higher concentrations of $CdCl_2$ resulted in a dose-dependent reduction of cell growth and viability.

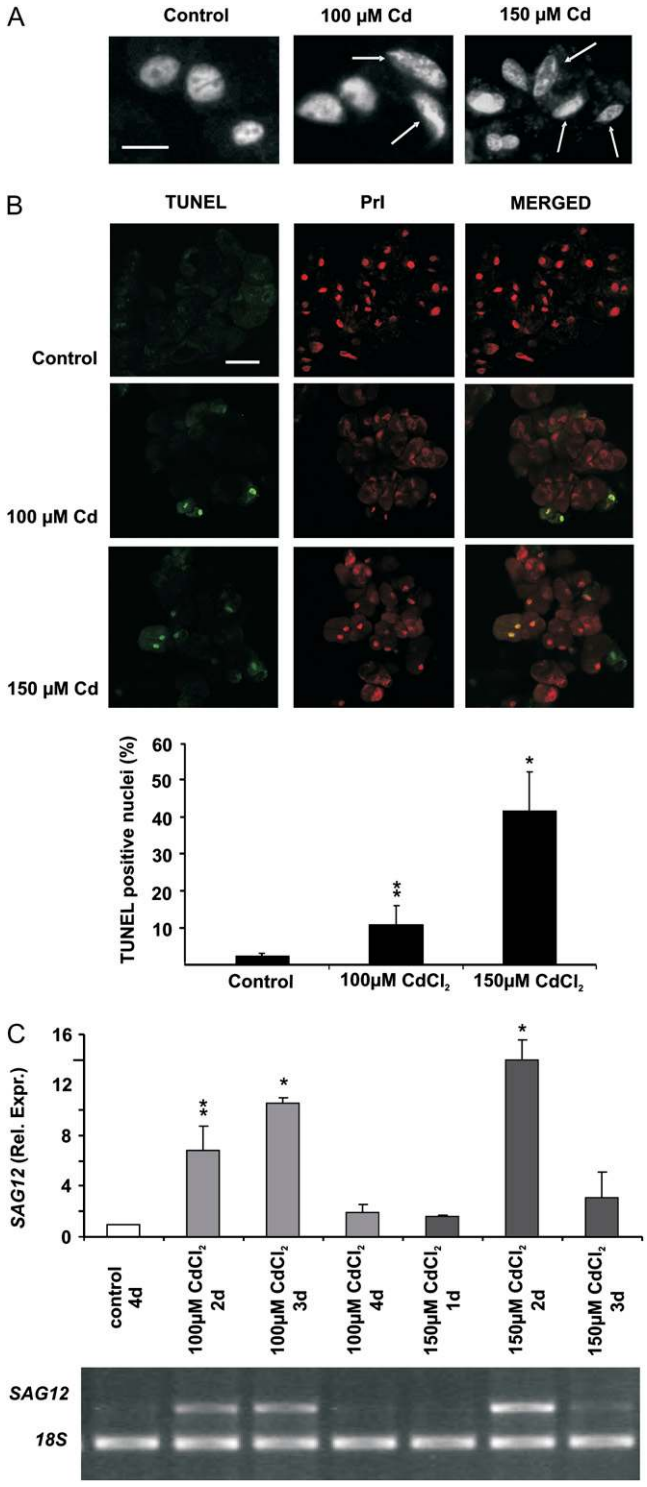

Figure 2. Characterization of cell death. A, Nuclei of untreated (control) cells and cells treated for 3 d with 100 or 150 μM $CdCl_2$, stained with DAPI. Arrows indicate typical nuclei with condensed, granular chromatin. Bar = 10 μm. B, TUNEL of cells treated for 4 d. Left column, Fluorescein; middle column, propidium iodide (PrI); right column, merged image. Bar = 30 μm. The graph at bottom presents the proportions of nuclei that scored positive for fluorescein. C, Expression of *SAG12*. The gel is representative of a typical RT-PCR experiment. Values in the graph represent ratios between pixel intensities of the *SAG12* and *18S* signals normalized against untreated cells (control), which are given a value of 1 and therefore have no SD. Asterisks indicate values that are significantly different from those of untreated cells by Student's *t* test (* $P < 0.01$, ** $P < 0.05$).

About 80% of the cells were dead at 7 and 4 d after treatment with 100 and 150 μM $CdCl_2$, respectively. Cl^- was not responsible for the toxic effects, as treatment with 150 μM $MgCl_2$ did not induce any change in the physiological parameters (data not shown). Since we were mainly interested in the events preceding cell death, all subsequent analyses were restricted to the first 3 to 4 d following treatment.

To determine if Cd^{2+} ions were able to enter the cells, we measured their internal concentration by atomic absorption spectrometry. The amount of Cd^{2+} inside the cells correlated with the dose of treatment. Cells growing for 3 d in a medium supplemented with 50 μM $CdCl_2$ contained 1.33×10^{-1} nmol mg^{-1} dry weight ($\pm 3.19 \times 10^{-2}$ SD) Cd^{2+}, whereas treatments with concentrations of 100 and 150 μM resulted in 3.04 nmol mg^{-1} dry weight ($\pm 9.15 \times 10^{-1}$ SD) and 7.09 nmol mg^{-1} dry weight ($\pm 2.72 \times 10^{-1}$ SD) internal Cd^{2+}, respectively.

In the presence of Cd^{2+}, plants produce PCs using reduced glutathione (GSH) as a substrate. To assess if Arabidopsis cell cultures similarly activate the same defense mechanism, we measured the content of PCs and GSH in cells treated with 50, 100, and 150 μM $CdCl_2$ (Fig. 1, C and D; Supplemental Fig. S1). As expected, untreated cells had nearly undetectable levels of PCs. Cd^{2+} triggered the formation of PCs at 7 h after treatment in a dose-dependent way. At a concentration of 150 μM $CdCl_2$, the maximum PC content was reached at 24 h, then it gradually decreased. At 100 μM, the peak was lower, but it was maintained up to 48 h after treatment. With 50 μM $CdCl_2$, the content of PCs was moderate but sustained for a longer period. Conversely, the levels of GSH severely decreased over time regardless of the $CdCl_2$ concentration used (Fig. 1D).

In order to test the role of PCs in protecting Arabidopsis cells from Cd^{2+} stress, we prevented their production in cells exposed to the sublethal dose of 50 μM $CdCl_2$ by pretreating with L-buthionine-sulfoximine (BSO), an inhibitor of the synthesis of GSH. As expected, when BSO was present, treatment with 50 μM $CdCl_2$ was not able to trigger the synthesis of PCs (Fig. 1C) and the content of GSH remained extremely low (Fig. 1D). Treatment with either BSO or 50 μM $CdCl_2$ alone had no effect on cell growth and viability (Fig. 1, A and B), whereas combined treatment determined a dramatic and rapid inhibition of growth and an increase in mortality. These data indicate that PCs have a primary role in Cd^{2+} detoxification.

Cd^{2+} Induces PCD by Accelerating Senescence

Cell death can occur by either necrosis or PCD. Generally, an early sign of PCD is the condensation of

chromatin (Clarke et al., 2000). In order to assess the nature of the death event induced by $CdCl_2$, we analyzed the nuclear morphology by 4′,6-diamidino-2-phenylindole (DAPI) staining (Fig. 2A). Untreated healthy cells showed round, uniformly stained nuclei with a large central nucleolus. By contrast, 3 d of treatment with 100 μM $CdCl_2$ caused chromatin condensation in a fraction (about 20%) of the cells, whose nuclei appeared stretched and with an irregular, granular staining. The proportion of this type of nuclear morphology increased in cells treated with 150 μM $CdCl_2$ (about 50%).

Another marker of PCD is the internucleosomal fragmentation of DNA, and the resulting 3′OH ends can be marked by the TUNEL assay (Fig. 2B). After 4 d of treatment with 100 μM $CdCl_2$, about 11% of nuclei appeared TUNEL positive, and the percentage increased to 45% when the $CdCl_2$ concentration was 150 μM. Conversely, nearly all of the nuclei of control cells were TUNEL negative.

To characterize further the events preceding cell death, we analyzed the expression of *senescence-associated gene12* (*SAG12*). This gene is considered the best molecular marker of senescence in Arabidopsis, as it is induced solely during this process (Noh and Amasino, 1999). Arabidopsis cell suspension cultures proved to be a suitable system in which to study senescence, as they express *SAG12* at the end of their growth cycle if the medium is not renewed (Carimi et al., 2004). At 100 μM, $CdCl_2$ determined an induction of *SAG12* at 2 and 3 d after treatment (Fig. 2C). At 4 d, when the cells started to die, the expression of the gene decreased. With a 150 μM treatment, this expression pattern occurred earlier and was more intense. These results indicate that under these experimental conditions, Cd^{2+} triggered a senescence-like process that eventually ended with PCD.

Signal Molecules in Cd^{2+} Toxicity: The Roles of Hydrogen Peroxide and NO

Reactive oxygen and nitrogen species, such as hydrogen peroxide (H_2O_2) and NO, are often produced in large quantities by plants during various stress responses, and they can also participate in signaling events leading to cell death. For these reasons, we investigated the involvement of these molecules in our system.

Measurements of H_2O_2 released in the culture medium revealed undetectable levels in untreated cells and in cells treated for up to 3 d with 50 μM $CdCl_2$ (Fig. 3A). At higher concentrations, we observed a dose dependence in the initiation and intensity of H_2O_2 production. Treatment with 100 μM $CdCl_2$ resulted in an increase in H_2O_2 content at 72 h after treatment. At a concentration of 150 μM $CdCl_2$, H_2O_2 levels increased at just 48 h after treatment and remained high the following day.

A different situation was recorded for NO release, as measured by fluorescence of the specific probe 4,5-diaminofluorescein (DAF-2). Within the first day following treatment with $CdCl_2$, NO levels remained low and just above the typical amount of untreated cells (Fig. 3B). After 24 h, the quantity of NO in cells treated with 50 μM $CdCl_2$ was about 2.5-fold that in control cells, and with doses of 100 and 150 μM $CdCl_2$, the increase was 4-fold. At subsequent times, NO decreased in cells treated with 50 μM $CdCl_2$, whereas it remained high or even increased at higher $CdCl_2$ concentrations. Only 72 h after treatment, NO decreased, most markedly with 150 μM $CdCl_2$. A similar pattern was also observed by recording the NO production inside the cells, by means of the internal fluorophore diaminofluorescein-FM-diacetate (DAF-FM-DA; Supplemental Fig. S2).

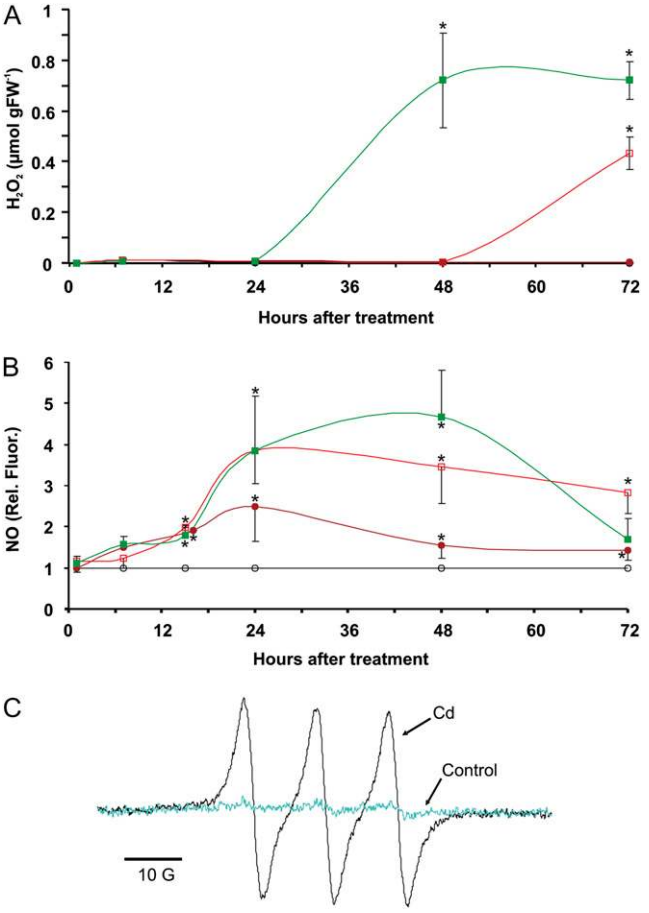

Figure 3. H_2O_2 and NO released by Arabidopsis cells after $CdCl_2$ treatment. Open circles, Control; closed circles, 50 μM $CdCl_2$; open squares, 100 μM $CdCl_2$; closed squares, 150 μM $CdCl_2$. A, H_2O_2 in culture medium was measured at different times after treatment with 50, 100, or 150 μM $CdCl_2$. Values are expressed as μmol per gram fresh weight (FW). B, NO released, measured by the DAF-2 method. Values are normalized against the levels of untreated cells (control), which are given a value of 1 and therefore have no SD. Asterisks indicate values that are significantly different from those of untreated cells by Student's *t* test (* $P < 0.01$). C, EPR spectra of the $(MGD)_2Fe(II)NO$ complex in cells treated with 150 μM $CdCl_2$ for 48 h and untreated cells (control). [See online article for color version of this figure.]

Cd^{2+}-induced NO production was confirmed by electron paramagnetic resonance (EPR) spectroscopy. The detection was performed with the NO-specific spin trap Fe(II) plus *N*-methyl-D-glucamine complex [$(MGD)_2Fe(II)$; Vanin and van Faassen, 2007]. Cells treated for 48 h with 150 μM $CdCl_2$ clearly presented the typical hyperfine structure triplet of the NO complex, whereas untreated cells exhibited only a faint signal, indicating that Cd^{2+} exposure led to a strong NO production (Fig. 3C).

Prevention of NO Synthesis Decreases Cd^{2+} Cytotoxicity

Under our experimental conditions, NO production was an early event preceding H_2O_2 release and cell death; thus, it constitutes a possible candidate as a signaling modulator of Cd^{2+}-induced PCD. To test this hypothesis, we pretreated the cells with N^G-monomethyl-Arg monoacetate (L-NMMA), an inhibitor of animal NOS that proved to be effective also in plant systems (Foissner et al., 2000; Garcês et al., 2001; Carimi et al., 2005). After an initial small increase in NO production due to the treatment with L-NMMA, probably due to a stress response, the presence of the NOS inhibitor markedly lowered the Cd^{2+}-induced NO production in cultures treated with 100 and 150 μM $CdCl_2$ (Fig. 4, A and B). L-NMMA also diminished the intracellular Cd^{2+}-induced NO synthesis, as observed by staining with DAF-FM-DA (Supplemental Fig. S2).

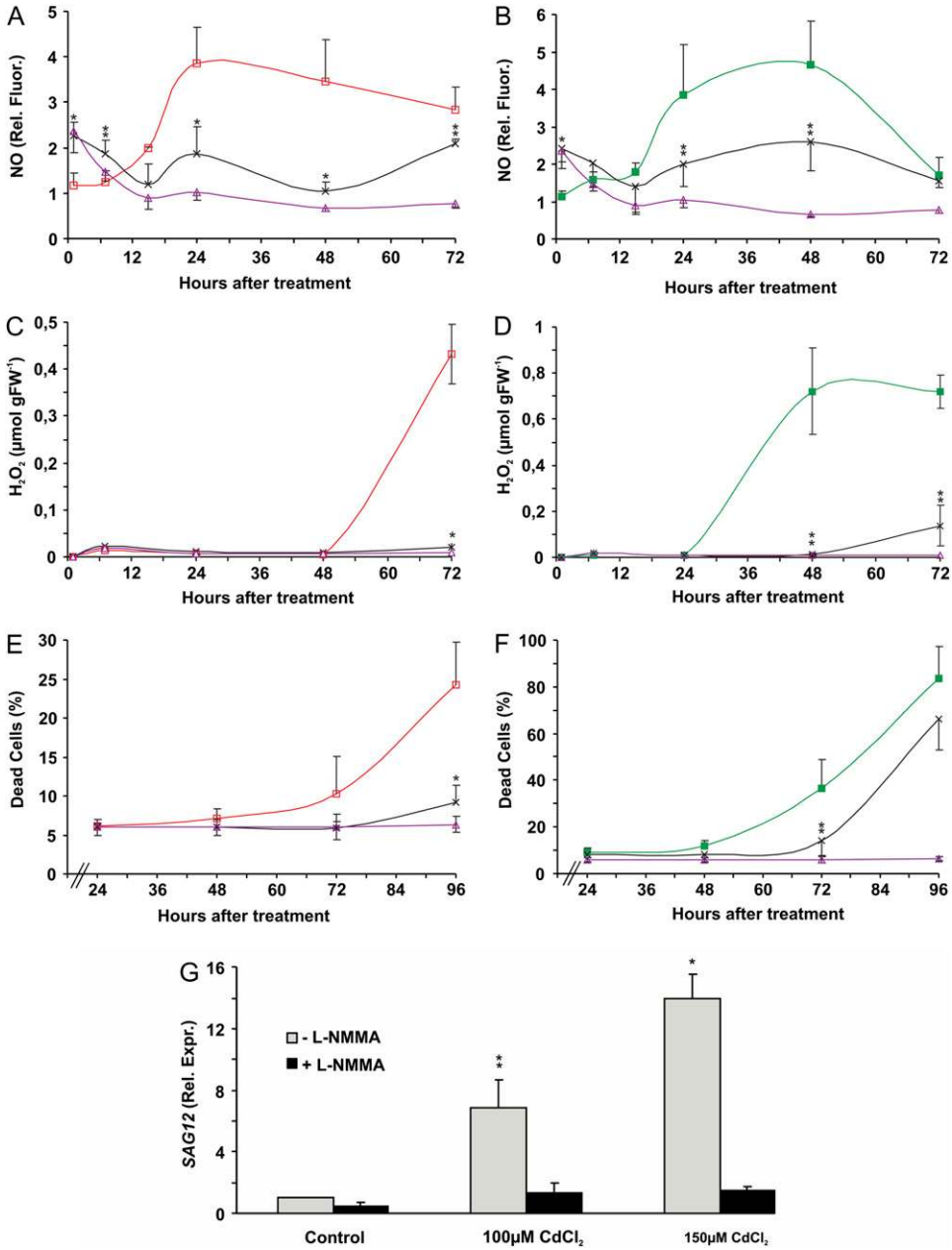

Figure 4. Effects of pretreatment with L-NMMA on NO and H_2O_2 levels, cell viability, and *SAG12* expression of cells treated with 100 μM $CdCl_2$ (A, C, and E) or 150 μM $CdCl_2$ (B, D, and F). Open triangles, L-NMMA; open squares, 100 μM $CdCl_2$; closed squares, 150 μM $CdCl_2$; crosses, 100 or 150 μM $CdCl_2$ + L-NMMA. A and B, NO released, measured with the DAF-2 method. Values were normalized against the levels of untreated cells (data not shown). C and D, H_2O_2 released in culture medium. FW, Fresh weight. E and F, Cell viability (Evans blue staining). G, Expression of *SAG12* at 2 d after treatment. Values were normalized against untreated cells, which are given a value of 1 and therefore have no SD. Asterisks indicate values that are significantly different from those of cells treated with the corresponding dose of $CdCl_2$ but not with L-NMMA by Student's *t* test (* $P < 0.01$, ** $P < 0.05$). [See online article for color version of this figure.]

Pretreatment with L-NMMA had a dramatic effect on extracellular H_2O_2 levels. The inhibitor completely prevented H_2O_2 production caused by treatment with 100 μM $CdCl_2$ and reduced it 5-fold at 72 h after treatment with 150 μM $CdCl_2$ (Fig. 4, C and D).

The protective effect of L-NMMA was also observed as a delay in mortality. The number of dead cells was reduced by the inhibitor from about 25% to 10% at 96 h after treatment with 100 μM $CdCl_2$ and from about 40% to 13% at 72 h after treatment with 150 μM $CdCl_2$ (Fig. 4, E and F).

Finally, we analyzed *SAG12* expression to monitor how a reduction of NO production affected the senescence process triggered by $CdCl_2$. We detected a strong reduction of the expression of the marker gene when pretreatment with L-NMMA was performed; in particular, 2 d after treatment with 100 or 150 μM $CdCl_2$, *SAG12* expression was reduced about 3.5- or 7-fold, respectively, in the presence of the inhibitor (Fig. 4G).

NO Affects Catalase and Ascorbate Peroxidase Activities in Vivo

The strong effect of L-NMMA on extracellular H_2O_2 levels might be caused by a modulation by NO of the antioxidant activities of some key enzymes. In particular, it has been demonstrated that, in vitro, NO is able to reversibly inhibit the heme-containing tobacco proteins catalase (CAT) and ascorbate peroxidase (APX), the two major enzymes in H_2O_2 detoxification (Clark et al., 2000). To test if the NO produced by $CdCl_2$ treatment in Arabidopsis cells similarly had an effect on the H_2O_2-scavanging capacity of CAT and APX, we measured changes in their activity when a pretreatment with L-NMMA was performed. We focused on the dose of 150 μM $CdCl_2$ because of the stronger response in terms of NO and H_2O_2 production. As shown in Figure 5, CAT activity increased when cells were treated with $CdCl_2$ for 1 to 2 d and returned to control levels at 3 d. However, an additional pretreatment with L-NMMA augmented CAT activity at any time of analysis. The activity of APX was not affected by $CdCl_2$ treatment in the first 2 d but was strongly decreased at longer incubation times. Still, this reduction was partly prevented if the NOS inhibitor was also present. These results indicate that NO production negatively affects the CAT and APX capacity of Cd^{2+}-treated cells.

Phytochelatins Are Regulated by NO

Considering the importance of PCs in protecting cells from Cd^{2+} toxicity, we wondered if modulation in NO levels had an effect on PC content. Pretreatment with L-NMMA increased the amount and extended over time the PC level in cells treated with 100 or 150 μM $CdCl_2$ (Fig. 6A). In fact, PC contents of cells treated for 48 h with 100 or 150 μM $CdCl_2$ were about 35% and 115% higher, respectively, when the NOS inhibitor was also present.

The chemical structure of PCs contains repetitions of the dipeptide Glu-Cys. NO is able to react with Cys residues (*S*-nitrosylation), especially when these are surrounded by acidic amino acids like Glu (Stamler et al., 1997), and NO reacts rapidly with glutathione, the precursor of PCs, to form *S*-nitrosoglutathione. Therefore, we hypothesized that PCs might similarly be nitrosylated. Liquid chromatography electrospray ion-trap mass spectrometry (LC-ESI-IT-MS) analysis of the PCs extracted from cells treated for 24 h with 150 μM $CdCl_2$ revealed that a fraction of them was mononitrosylated in their Cys residues. The most abundant *S*-nitrosylated PCs were identified on the basis of either the full-scan mass spectra exhibiting the presence of the protonated molecular ions $[(M)^+]$ or the product-ion mass spectra showing the loss of –30 D $[(M\text{-}30)^+]$ attributable to the NO group (Fig. 6B). Importantly, the total amount of nitrosylated PCs de-

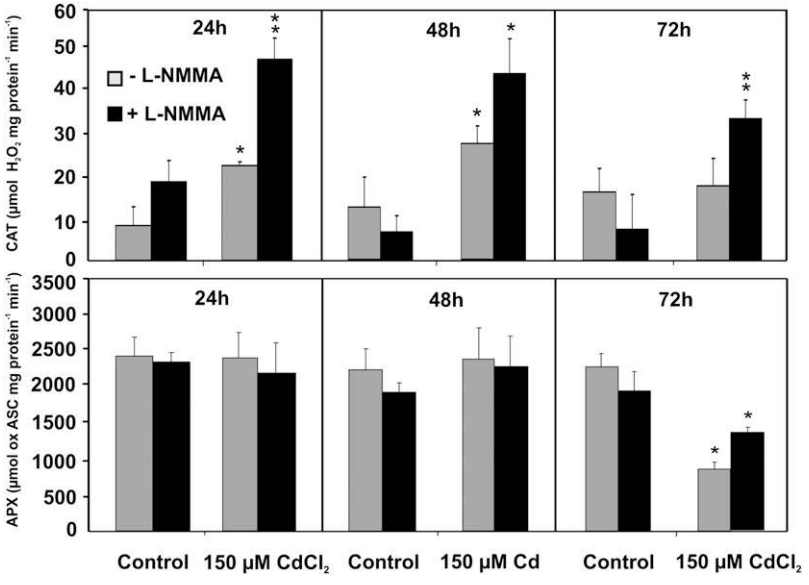

Figure 5. Effects of L-NMMA on CAT and APX activity of untreated cells and cells treated with 150 μM $CdCl_2$. Asterisks indicate values that are significantly different from those of either untreated cells (150 μM $CdCl_2$) or cells treated with $CdCl_2$ but not with L-NMMA (150 μM $CdCl_2$ + L-NMMA) by Student's *t* test (* $P < 0.01$, ** $P < 0.05$).

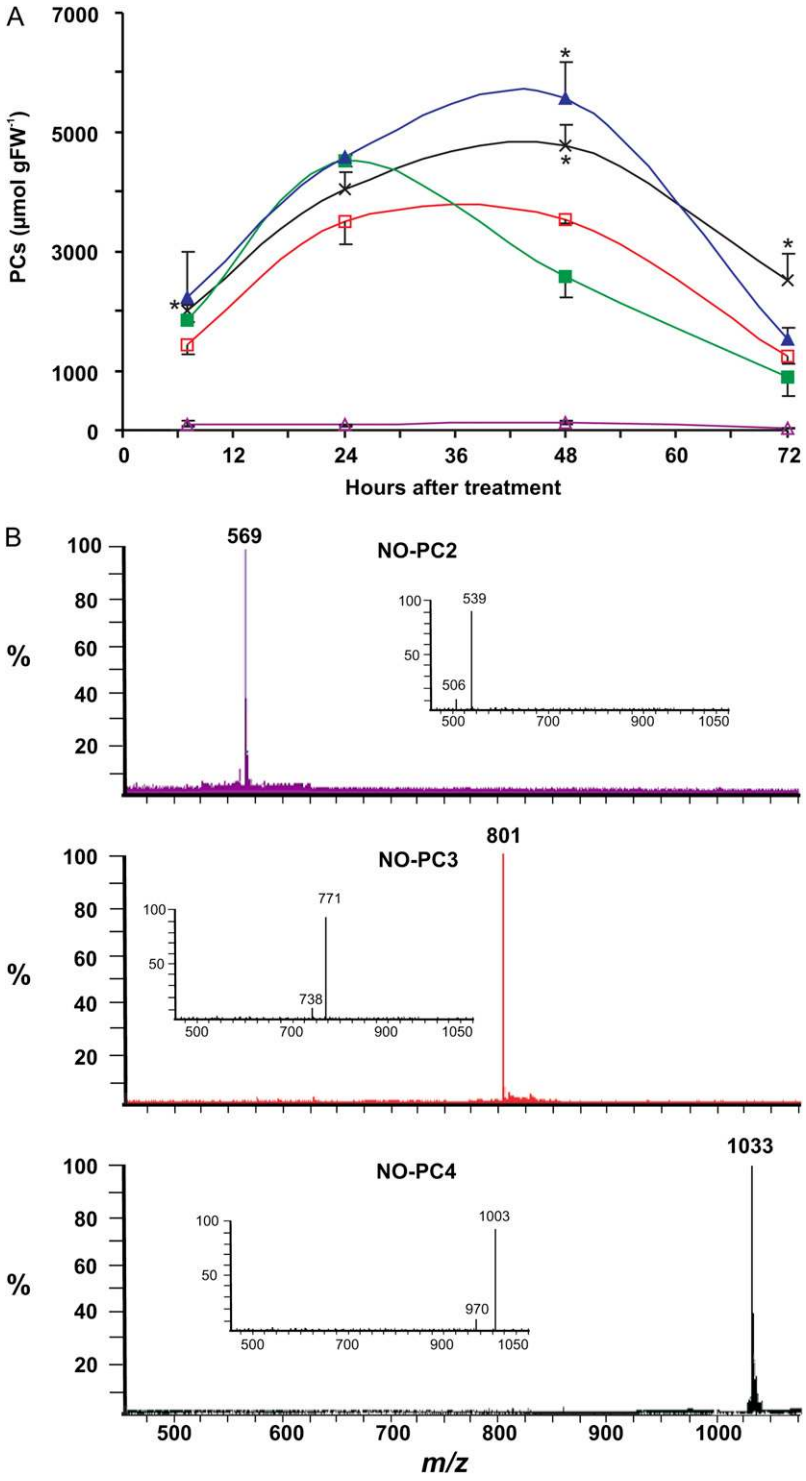

Figure 6. Effects of NO on total PC content and structure. A, PC content of cells pretreated with L-NMMA and treated with 100 or 150 μM $CdCl_2$. Open triangles, L-NMMA; open squares, 100 μM $CdCl_2$; closed squares, 150 μM $CdCl_2$; crosses, 100 μM $CdCl_2$ + L-NMMA; closed triangles, 150 μM $CdCl_2$ + L-NMMA. Asterisks indicate values that are significantly different from those of cells treated with the corresponding dose of $CdCl_2$ but not with L-NMMA by Student's *t* test (* $P < 0.05$). FW, Fresh weight. B, LC-ESI-MS full-scan mass spectra of mononitrosylated PCs extracted by cells treated for 24 h with 150 μM $CdCl_2$. Protonated molecular ions $[(M+H)^+]$ at m/z = 569 for NO-PC_2, 801 for NO-PC_3, and 1,033 for NO-PC_4. The insets show their corresponding fragmentation patterns exhibiting the loss of the nitro moiety $[(M+H-30)^+]$. [See online article for color version of this figure.]

creased by about 50% (±15 SD) when the cells were pretreated with L-NMMA (Supplemental Fig. S3).

DISCUSSION

Exposure to Cd^{2+} leads to various alterations in plant homeostasis and can even result in cell death, but the molecular mechanisms of Cd^{2+} cytotoxicity are currently uncertain. Most previous studies have employed high (millimolar) concentrations of Cd^{2+}, and with these treatments, cell death occurred within a few hours (Piqueras et al., 1999; Olmos et al., 2003; Garnier et al., 2006). However, these experimental conditions do not reflect a typical situation found in contaminated soils, where concentrations of Cd^{2+} are usually much lower (Sanità di Toppi and Gabbrielli, 1999). Moreover,

it has been observed that in tobacco cell cultures and onion root apical cells, high doses of Cd^{2+} induce a necrotic type of cell death. On the contrary, in those systems, the process of cell death resulting from treatment with 50 μM Cd^{2+} is slower and shows characteristics typical of PCD (Fojtovà and Kovařik, 2000; Behboodi and Samadi, 2004). In our conditions, Arabidopsis cell cultures were more tolerant to $CdCl_2$ than tobacco BY2 and onion root cells, as treatment with 50 μM $CdCl_2$ had virtually no effect on growth and viability. At higher doses, however, a process of PCD was triggered, as indicated by the condensation of the chromatin, its cleavage in oligonucleosomal segments, and the premature expression of the senescence marker *SAG12*. Senescence is considered a particular type of PCD, and its initiation can be regulated by several biotic and abiotic stresses (Buchanan-Wollaston et al., 2003). Morphological and biochemical observations had already suggested that an effect of chronic exposure of plants to Cd^{2+} was precocious senescence (Rascio et al., 1993; McCarthy et al., 2001; Sandalio et al., 2001; Rodriguez-Serrano et al., 2006). Interestingly, *SAG12* is the gene with the highest induction in a transcriptomic analysis of Arabidopsis plants treated for 21 d with 50 μM Cd^{2+} (Kovalchuk et al., 2005). The results presented in this work corroborate these observations at the molecular level and define a dose dependence in the timing and intensity of the onset of the senescence process and of the final cell death event.

Plants rapidly respond to Cd^{2+} by producing PCs, which bind the toxic free metal ions and dispose of them into the vacuole. Likewise, Cd^{2+} stimulates the synthesis of PC precursors, GSH and Cys, to sustain PC production (Dominguez-Solis et al., 2001; Howarth et al., 2003). We found a clear dose dependence in the levels of PCs synthesized, which correlates well with the different amounts of Cd^{2+} inside the cells. PCs proved to be of primary importance in the defense strategy against $CdCl_2$ toxicity, as inhibition of their synthesis resulted in an abrupt sensitivity to the otherwise sublethal dose of 50 μM. A paucity of GSH per se is not sufficient to induce cell death, as GSH depletion following treatment with 50 μM $CdCl_2$ was roughly similar to that caused by higher, lethal doses.

To date, little information is available about the signaling pathways involved in Cd^{2+}-induced PCD. On the other hand, several studies have focused on the importance of ROS production after treatment with high concentrations of $CdCl_2$, which rapidly causes necrosis of exposed cells (Piqueras et al., 1999; Olmos et al., 2003; Garnier et al., 2006). Recently, a rapid production of H_2O_2 was also reported for Arabidopsis cell cultures treated with 10 to 75 μM Cd^{2+} (Horemans et al., 2007). However, that study was not focused on Cd^{2+} cytotoxicity and its signaling events, and we show that concentrations up to 50 μM are ineffective at inducing cell death. In our system, we observed an increase in the extracellular H_2O_2 levels only when cultures were exposed to PCD-inducing $CdCl_2$ concentrations (100 and 150 μM). At both doses, the increase in H_2O_2 levels was a late event and preceded cell death by about 24 h. Such timing suggests that this ROS production is part of the degenerative stage eventually leading to cell death, rather than a genuine signaling event. Similarly, delayed oxidative stress was also detected in leaves and roots of pea plants treated for 14 d with 50 μM Cd^{2+}, and indeed, a large part of these tissues appeared already dead at the moment of analysis (Romero-Puertas et al., 2004; Rodriguez-Serrano et al., 2006). It must be noted, however, that our assay measured only H_2O_2 released in the culture medium, and we cannot exclude a milder, earlier intracellular production, which may be scavenged before passing the cell wall. Although Cd^{2+} is not able to directly generate ROS by a Fenton reaction, it might inhibit antioxidant enzymes, impair the respiratory chain, or displace copper and iron ions in metalloproteins, which eventually trigger a Fenton reaction (Valko et al., 2005, and refs. therein). Cd^{2+}-induced H_2O_2 might be produced by plasma membrane NADPH oxidase (Garnier et al., 2006; Ortega-Villasante et al., 2007) or originate in mitochondria and then diffuse to other parts of the cells and in the apoplastic space (Heyno et al., 2008). The plant response to Cd^{2+} in terms of antioxidant activities varies greatly, depending on the enzyme, the plant species, the tissue analyzed, the plant age, the intensity of the Cd^{2+} treatment, and its duration (Schutzendubel and Polle, 2002). In our conditions, we found that 150 μM $CdCl_2$ increased the activity of CAT up to 2 d of treatment. However, the late production of H_2O_2 at 2 and 3 d after $CdCl_2$ addition, when cells started to die, indicates that at this stage the antioxidant machinery was not able to cope with the oxidative stress, and accordingly, we observed a marked reduction in APX activity at 3 d of treatment.

Cell cultures proved to be an effective system to unravel the role of NO in the signaling of many PCD events, from the hypersensitive response to senescence

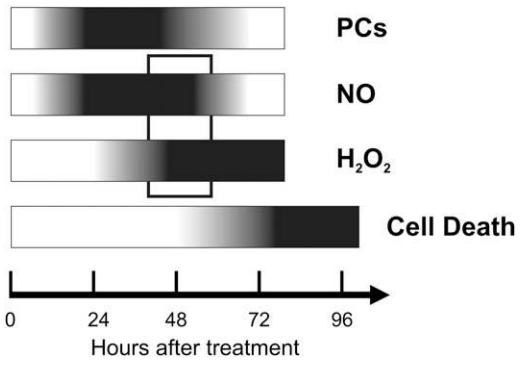

Figure 7. Time scale of events following treatment with 150 μM $CdCl_2$. The intensity of the shading of the bars corresponds to the levels of PCs, NO, H_2O_2, and cell death. The rectangle represents the time window in which both NO and H_2O_2 occur. These events in cells treated with 100 μM $CdCl_2$ follow a similar pattern but occur later (data not shown).

(Delledonne et al., 1998; Carimi et al., 2005). In this work, we show that NO is also involved in Cd^{2+}-induced PCD, and this finding correlates well with the hypothesis of accelerated senescence. NO was produced about 24 h after treatment with 100 and 150 μM $CdCl_2$, and its levels remained high as long as cells were viable. A similar trend was observed in roots of pea and *Brassica juncea*, where NO levels increased at 1 to 5 d after treatment with 100 μM Cd^{2+} (Bartha et al., 2005). Conversely, a 2-week exposure of pea roots to 50 μM Cd^{2+} lowered levels of NO (Rodriguez-Serrano et al., 2006); however, at this stage, a large part of the root tissue appeared dead, and thus it is likely that such a time point is too late to record an early NO production. A new finding of this work, to our knowledge, is that NO is actually required for Cd^{2+}-induced PCD, as prevention of its synthesis had a positive effect on cell viability and lowered the expression of *SAG12*. Moreover, our experiments revealed that after $CdCl_2$ treatment, NO is produced via NOS-like activity, as L-NMMA is a specific inhibitor of this route of synthesis. We postulate that NO is linked to ROS production, which eventually leads to cell death. To date, little evidence has suggested NO-dependent H_2O_2 formation (Clark et al., 2000); an increase in H_2O_2 production following treatment with a NO donor was detected in Arabidopsis plants (Murgia et al., 2004). A possible causal mechanism is the ability of NO to inhibit the antioxidant enzymes CAT and APX (Clark et al., 2000; Murgia et al., 2004); in rat mitochondria, CAT can actually be nitrosylated (Foster and Stamler, 2004). Interestingly, we found that in cells treated with 150 μM $CdCl_2$, the activities of CAT and APX increased when L-NMMA was also present, and this could explain the effect of the NOS inhibitor in lowering H_2O_2 levels.

Prevention of NO synthesis had a significant, positive effect on the levels of PCs. However, at present, we are not able to discern whether a higher PC content is responsible for the delay in cell death or if it may be a consequence of the healthier status of the cells. A mechanism through which NO might modulate the PC capability to chelate Cd^{2+} is by direct nitrosylation. We found that part of the PCs extracted from cells treated with 150 μM $CdCl_2$ for 24 h showed a specific nitrosylation signature when analyzed with MS. Moreover, the extent of nitrosylation halved in the presence of the NOS inhibitor, a decrease that overlapped that of NO production. As both Cd^{2+} and NO bind to the Cys residues of PCs, nitrosylated PCs are probably less effective at chelating Cd^{2+}; therefore, the free ions would be able to exert their toxic effects. Supporting this hypothesis is the finding that metallothioneins, when nitrosylated, release Cd^{2+} and Zn^{2+} and NO donors increase Cd^{2+} toxicity in animal cells (Misra et al., 1996; Katakai et al., 2001). As metallothioneins can be functionally considered the animal counterpart of PCs and also bind metal ions through their Cys residues (Cobbett, 2000), it is likely that a similar situation occurs in plant PCs.

The events that follow treatment of Arabidopsis cell culture with 150 μM $CdCl_2$ are summarized in Figure 7. The first response is a rapid production, within 1 d, of PCs and NO. Their concomitant presence explains the pattern of nitrosylated PCs and corroborates the hypothesis of a control of PC content/function by NO. H_2O_2 intervenes at later times, preceding the rise of cell death at about 24 h. Experiments with H_2O_2 and NO donors in cell cultures have shown that cell death follows the bursts of reactive species at about 6 to 24 h (de Pinto et al., 2002, 2006; Zottini et al., 2002). It is noteworthy that, about 2 d after treatment with 150 μM $CdCl_2$, levels of both NO and H_2O_2 are high. It has long been suggested that these two players cooperate in triggering PCD events, such as the hypersensitive response (Delledonne et al., 2001; de Pinto et al., 2006). The requirement for concurrent NO and H_2O_2 would explain why 50 μM $CdCl_2$ is not toxic; at this concentration, NO production is low and transitory, and it is never accompanied by a H_2O_2 burst.

In conclusion, in this work, we define the timing and conditions of PCD induced by moderate $CdCl_2$ treatments, and we describe in detail some of the events characterizing this process. The finding that NO plays a key role in the regulation of Cd^{2+} cytotoxicity opens novel possibilities for increasing plant tolerance to heavy metals and phytoremediation.

MATERIALS AND METHODS

Cell Cultures and Treatments

Suspension cell culture was generated from hypocotyls dissected from young plantlets of Arabidopsis (*Arabidopsis thaliana* ecotype Landsberg *erecta*) and subcultured in AT3 medium (Desikan et al., 1996). For subculture cycles, 0.6 mL of packed cell volume was placed in 100-mL Erlenmeyer flasks containing 20 mL of liquid medium. Cells were subcultured in fresh medium at 7-d intervals and maintained in a climate chamber on a horizontal rotary shaker (80 rpm) at 25°C ± 1°C with a 16-/8-h photoperiod and a light intensity of 70 μmol m^{-2} s^{-1}. Treatments with filter-sterilized solutions of $CdCl_2$, L-NMMA, and BSO were carried out with 3-d-old cultures. L-NMMA (1 mM; Alexis Biochemicals) and BSO (1 mM; Sigma-Aldrich), when required, were added at 1 h before $CdCl_2$ treatment.

Cell Viability and Analysis of Nuclear Morphology

Cell death was determined by spectrophotometric measurements of the uptake of Evans blue, as described by Gaff and Okong'o-Ogola (1971). Nuclei were visualized by staining with DAPI (Alexis Biochemicals) as described by Traas et al. (1992), with some modifications. An aliquot of 500 μL of suspension culture was added to an equal volume of fixation solution (4% [w/v] paraformaldehyde in PEM buffer: 100 mM HEPES, pH 6.9, 10 mM EGTA, and 10 mM $MgSO_4$). After 30 min, cells were washed three times in PEM buffer and resuspended in 500 μL of PEM buffer. An aliquot of 200 μL of fixed cells was then added to an equal volume of PEM buffer containing 0.2% (w/v) Triton X-100 and 1 μg mL^{-1} DAPI. Stained cells were laid on a glass slide treated with poly-L-Lys, and nuclei were visualized with a fluorescence microscope (DMR; Leica) with an excitation filter of 330 to 380 nm and a barrier filter of 410 nm.

TUNEL Assay

Cells undergoing PCD were detected with the Fluorescein In Situ Cell Death Detection Kit (Roche Diagnostic) according to the manufacturer's instructions. Briefly, cells were fixed in 4% formaldehyde, permeabilized with 0.1% Triton

X-100 and 0.1% sodium citrate, and incubated at 37°C for 60 min with terminal deoxynucleotidyl transferase and fluorescein-conjugated nucleotides. Slides were observed with a fluorescence microscope (DMR; Leica) with an excitation filter of 488 nm and an emission of 515 to 530 nm. Nuclei were stained with 5 μg mL^{-1} propidium iodide and visualized with emission spectra of 575 to 625 nm.

Internal Cd^{2+} Quantification

Cells were collected by centrifugation of 2 mL of suspension culture at 1,000*g* for 3 min. External Cd^{2+} was removed by washing the pellet two times with 10 mL of deionized water, two times with 10 mL of 10 mM EDTA, and finally two more times with 10 mL of deionized water. After each wash, cells were recollected by centrifugation and the supernatant was discarded. Cells were then dried for 24 h at 60°C and accurately weighed. Internal Cd^{2+} was released by incubation with 5 mL of 0.1 M HCl for 40 min at 50°C. Samples were read using an atomic spectrometer (Aanalyst; Perkin-Elmer), and concentration values were obtained using a calibration curve and normalizing for the dry weight.

H_2O_2 Quantification

Extracellular H_2O_2 was measured in culture medium as described by Bellincampi et al. (2000), with some modifications. Briefly, 1 mL of suspension culture was filtered through a chromatographic column (Poly-Prep; Bio-Rad) to separate cells from the growth medium. An aliquot of 500 μL of the flow-through was added to an equal volume of assay reagent (500 μM ferrous ammonium sulfate, 50 mM H_2SO_4, 200 μM xylenol orange, and 200 mM sorbitol) and incubated for 45 min in the dark. The H_2O_2-mediated oxidation of Fe^{2+} to Fe^{3+} was determined by measuring the A_{560} of the Fe^{3+}-xylenol orange complex. A calibration curve obtained by measuring the A_{560} of H_2O_2 standards allowed the conversion of the absorbance values into concentration estimates. All reactions were carried out at least in duplicate, and their reproducibility was checked. Values are expressed as micromoles of H_2O_2 per gram of fresh filtered cells (means ± SD).

NO Quantification by Fluorescence Analysis

Extracellular NO was determined by fluorimetric assay through its binding to the specific fluorophore DAF-2 (Alexis Biochemicals; Nakatsubo et al., 1998). Fluorescence measurements were performed with a LS-55 Luminescence Spectrometer (Perkin-Elmer) with an excitation wavelength of 495 nm and an emission wavelength of 515 nm, using a slit width of 3 nm. We followed the procedure of Carimi et al. (2005). NO was quantified as fold number compared with untreated cells (relative fluorescence). All reactions were carried out at least in duplicate, and their reproducibility was checked.

Intracellular NO was detected with the fluorescent dye DAF-FM-DA (Alexis Biochemicals). One milliliter of suspension culture was incubated with 0.5 μM DAF-FM-DA for 15 min at 25°C in a rotating plate agitator, and then cells were washed three times with 1 mL of AT3 medium. Fluorescence was estimated using a confocal laser scanning microscope (Nikon PCM2000) with an excitation of 488 nm and an emission of 515 to 530 nm.

NO Detection by EPR Analysis

NO released by cells was detected using the spin trap $(MGD)_2Fe(II)$ (Alexis Biochemicals). An aliquot of 950 μL of suspension culture was added to an equal volume of reaction buffer (1 mM $FeSO_4$, 10 mM MGD, and 25 mM phosphate buffer, pH 7.2) and incubated for 30 min in the dark on a rotatory shaker. After 3 min of centrifugation at 1,200*g*, 300 μL of supernatant was then added to 15 μL of reduction solution (1 M $Na_2S_2O_4$ in 2 M phosphate buffer, pH 7.2). EPR spectra were recorded using a Bruker ECS106 X-band spectrometer equipped with a Bruker TM4103 cavity. EPR experimental conditions were as follows: room temperature; microwave frequency, 9.79 GHz; microwave power, 20 mW; modulation amplitude, 1 G; time constant, 164 ms; conversion time, 82 ms; number of accumulations, five.

SAG12 Analysis

Cells were harvested, frozen in liquid N_2, and stored at −80°C. RNA isolation was carried out using Trizol (Invitrogen) following the manufacturer's instructions. The RNA preparations were treated with DNaseI (Ambion). Five micrograms of total RNA from each treatment was reverse transcribed using PowerScript reverse transcriptase (BD Biosciences) following the manufacturer's instructions and then diluted 5-fold with distilled water. Five microliters of this diluted cDNA was amplified by reverse transcription (RT)-PCR, according to the manufacturer's instructions (Taq DNA Polymerase). The *18S* rRNA primers and competimers of the Quantum RNA Universal 18S Internal Standards Kit (Ambion) were used as an internal standard. The primers used for the RT-PCR analysis of SAG12 were 5′-ACTGGAGGAAGAAAGGAGCTGT-3′ (forward) and 5′-TGATCCGTTAGTAGATTCGCGT-3′ (reverse). The following cycle conditions were used: 94°C for 30 s, followed by 36 cycles at 94°C for 20 s, 66°C for 45 s, and 72°C for 45 s, using a Hybaid PCR express thermal cycler. Electrophoresis of the PCR products was carried out on 1.5% (w/v) agarose gels containing 1× Tris-acetate-EDTA buffer, and products were visualized by ethidium bromide staining. Pixel intensities were then quantified with ImageJ software (National Institutes of Health), and *SAG12* values were normalized with the corresponding *18S* intensities. Expression values are presented as fold number compared with untreated 4-d-old cells (relative expression).

Enzyme Assays

Protein extraction was carried out at 4°C. About 3 mL of packed cells was ground in a mortar with sand and 5 mL of extraction buffer, which in the case of the CAT assay consisted of 0.1 M Tris-HCl, pH 7.5, 2 mM phenylmethylsulfonyl fluoride, 1 mM benzamidine, and 2 μg mL^{-1} aprotinin. Proteins for the APX assay were extracted with 50 mM potassium phosphate buffer, pH 7, and 1 mM sodium ascorbate. Homogenate was centrifuged at 16,000*g* for 2 min. The protein concentration in the supernatant was estimated by means of the Bio-Rad Protein Assay and adjusted with the extraction buffers to yield a similar concentration among the samples. Enzymatic activities were tested with a Cary 100 Bio UV-Visible spectrophotometer (Varian). Direct addition of 150 μM $CdCl_2$ to protein extracts up to 10 min prior of assays did not vary CAT or APX activities. CAT activity was determined by measuring the decrease in H_2O_2 A_{240}, as described by Aebi (1984), with some modifications. The assay was performed at 25°C in a 2-mL reaction mixture containing 10 mM H_2O_2, 50 mM phosphate buffer, pH 7, and 25 μg of proteins. The activities were estimated with an extinction coefficient of 39.4 mM^{-1} cm^{-1} and expressed as micromoles of H_2O_2 disproportionation per minute per milligram of protein. The activity of APX was measured following the H_2O_2-dependent oxidation of ascorbate as decrease of A_{290}, as described by Amako et al. (1994), with some modifications. The assay was performed at 25°C in a 2-mL reaction mixture containing 500 μM sodium ascorbate, 100 μM H_2O_2, 50 mM phosphate buffer, pH 7, and 50 μg of proteins. The rates of the reaction were corrected for spontaneous ascorbate oxidation in the absence of H_2O_2. The activities were estimated with an extinction coefficient of 2.8 mM^{-1} cm^{-1} and expressed as micromoles of ascorbate oxidized per minute per milligram of protein. The presence of ascorbate in the extraction buffer allowed the recovery of both the cytosolic and plastidial APX isoforms, the latter being very unstable in the absence of ascorbate (Shigeoka et al., 2002). The reported values, therefore, refer to the total APX activity in the extracts.

Quantification of PCs and GSH

About 400 mg of cells was homogenized in a mortar in ice-cold 5% (w/v) 5-sulfosalicylic acid, containing 6.3 mM diethylenetriaminepentaacetic acid, according to De Knecht et al. (1994). After centrifugation at 10,000*g* for 10 min at 4°C, supernatants were filtered through Minisart 0.45-μm filters (Sartorius) and immediately assayed by reverse-phase HPLC (model 200; Perkin-Elmer). Thiol-containing peptides (GSH and PCs) were separated by a Purosphere reverse-phase C_{18} column (Merck) by injecting 200 μL of extract. Separation was obtained using a 0% to 26% (v/v) CH_3CN gradient with a flow rate set at 0.7 mL min^{-1}. Elution solutions contained 0.05% (v/v) trifluoroacetic acid. Thiol-containing peptides were determined using postcolumn derivatization with 300 μM Ellman's reagent [5,5′dithio(2-nitrobenzoic acid)]. They were detected at 412 nm and measured by a calibration curve for standard sulfhydryl groups. Identification of GSH and individual PCs was based on the comparison of their retention times with standard GSH (Merck) and PC samples from *Silene vulgaris* (Moench). Values were normalized by fresh weight.

Characterization of *S*-Nitrosylated Peptides by HPLC-MS and HPLC-MS/MS

Liquid chromatographic elution was carried out on the Gemini C18 110-Å column (100 × 2.0 mm, 3-μm particles; Phenomenex) using a gradient solvent

system (solvent A, aqueous 0.1% [v/v] trifluoroacetic acid; solvent B, 0.05% [v/v] trifluoroacetic acid in acetonitrile) as follows: solvent B was set at 5% for 2 min and then raised with a linear gradient to 95% in 21 min. Solvent B was maintained at 95% for 5 min before column reequilibration (10 min). The flow rate was 0.2 mL min^{-1}.

The mobile phase was delivered by a Surveyor chromatographic system (ThermoElectron) equipped with a 200-vial capacity sample tray. Injection volume was 50 μL.

A LTQ XL linear ion trap instrument (ThermoElectron) equipped with a pneumatically assisted ESI interface was used. The system was controlled by Xcalibur software. The sheath gas (nitrogen, 99.999% purity) and the auxiliary gas (helium, 99.999% purity) were delivered at the flow rates of 45 and 5 arbitrary units, respectively.

The optimized conditions of the interface were as follows: ESI voltage, 3.5 kV; capillary voltage, 20 V; capillary temperature, 200°C. MS experiments were carried out in the 400 to 1,300 mass-to-charge ratio (*m/z*) range. MS/MS experiments were performed under product-ion conditions with a collision gas pressure of 2.3×10^{-3} mbar in the collision cell in a *m/z* set as a function of PC molecular mass.

Statistics

All experiments were conducted at least in triplicate, and their means ± SD are presented. The nuclear assays (DAPI staining and TUNEL) were performed on 15 different slides per sample, each containing at least 20 cells. Statistical differences of mean values of either cells treated with $CdCl_2$ and untreated cells or Cd^{2+}-treated cells with or without L-NMMA were determined with Student's *t* test.

Supplemental Data

The following materials are available in the online version of this article.

Supplemental Figure S1. Contents of the different forms of PCs in cells exposed to 50, 100, or 150 μM $CdCl_2$.

Supplemental Figure S2. Internal NO production, assayed by DAF-FM-DA staining, in cells exposed to 50, 100, or 150 μM $CdCl_2$.

Supplemental Figure S3. HPLC-ESI-MS extract-ion chromatograms of Arabidopsis cells exposed for 24 h to 150 μM $CdCl_2$ and 150 μM $CdCl_2$ + L-NMMA.

ACKNOWLEDGMENTS

We are grateful to Barbara Baldan (University of Padova) for her help with the TUNEL assay and to Laura De Gara (University of Bari) and Mario Terzi (University of Padova) for helpful discussions.

Received November 28, 2008; accepted March 1, 2009; published March 4, 2009.

LITERATURE CITED

Aebi H (1984) Catalase in vitro. Methods Enzymol **105:** 121–126

Amako K, Chen GX, Asada K (1994) Separate assays specific for ascorbate peroxidase and guaiacol peroxidase and for the chloroplastic and cytosolic isoenzymes of ascorbate peroxidase in plants. Plant Cell Physiol **35:** 497–504

Bartha B, Kolbert Z, Erdei L (2005) Nitric oxide production induced by heavy metals in *Brassica juncea* L. Czern. and *Pisum sativum* L. Proceedings of the 8th Hungarian Congress on Plant Physiology and the 6th Hungarian Conference on Photosynthesis **49:** 9–12

Behboodi BS, Samadi L (2004) Detection of apoptotic bodies and oligonucleosomal DNA fragments in cadmium-treated root apical cells of *Allium cepa* Linnaeus. Plant Sci **167:** 411–416

Beligni MV, Fath A, Bethke PC, Lamattina L, Jones RL (2002) Nitric oxide acts as an antioxidant and delays programmed cell death in barley aleurone layers. Plant Physiol **129:** 1642–1650

Bellincampi D, Dipierro N, Salvi G, Cervone F, De Lorenzo G (2000) Extracellular H_2O_2 induced by oligogalacturonides is not involved in the inhibition of the auxin-regulated rolB gene expression in tobacco leaf explants. Plant Physiol **122:** 1379–1385

Besson-Bard A, Pugin A, Wendehenne D (2008) New insights into nitric oxide signaling in plants. Annu Rev Plant Biol **59:** 21–39

Buchanan-Wollaston V, Earl S, Harrison E, Mathas E, Navabpour S, Page T, Pink D (2003) The molecular analysis of leaf senescence: a genomics approach. Plant Biotechnol J **1:** 3–22

Carimi F, Terzi M, De Michele R, Zottini M, Lo Schiavo F (2004) High levels of the cytokinin BAP induce PCD by accelerating senescence. Plant Sci **166:** 963–969

Carimi F, Zottini M, Costa A, Cattelan I, De Michele R, Terzi M, Lo Schiavo F (2005) NO signalling in cytokinin-induced programmed cell death. Plant Cell Environ **28:** 1171–1178

Cho UH, Seo NH (2005) Oxidative stress in *Arabidopsis thaliana* exposed to cadmium is due to hydrogen peroxide accumulation. Plant Sci **168:** 113–120

Clark D, Durner J, Navarre DA, Klessig DF (2000) Nitric oxide inhibition of tobacco catalase and ascorbate peroxidase. Mol Plant Microbe Interact **13:** 1380–1384

Clarke A, Desikan R, Hurst RD, Hancock JT, Neill SJ (2000) NO way back: nitric oxide and programmed cell death in Arabidopsis thaliana suspension cultures. Plant J **24:** 667–677

Clemens S (2006) Toxic metal accumulation, responses to exposure and mechanism of tolerance in plants. Biochimie **88:** 1707–1719

Cobbett CS (2000) Phytochelatins and their roles in heavy metal detoxification. Plant Physiol **123:** 825–832

De Knecht JA, Van Dillen M, Koevoets P, Schat H, Verkleij J, Ernst W (1994) Phytochelatins in cadmium-sensitive and cadmium-tolerant *Silene vulgaris* (chain length distribution and sulfide incorporation). Plant Physiol **104:** 255–261

Delledonne M, Xia Y, Dixon RA, Lamb C (1998) Nitric oxide functions as a signal in plant disease resistance. Nature **394:** 585–588

Delledonne M, Zeier J, Marocco A, Lamb C (2001) Signal interactions between nitric oxide and reactive oxygen intermediates in the plant hypersensitive disease resistance response. Proc Natl Acad Sci USA **98:** 13454–13459

de Pinto MC, Paradiso A, Leonetti P, De Gara L (2006) Hydrogen peroxide, nitric oxide and cytosolic ascorbate peroxidase at the crossroad between defence and cell death. Plant J **48:** 784–795

de Pinto MC, Tommasi F, De Gara L (2002) Changes in the antioxidant systems as part of the signaling pathway responsible for the programmed cell death activated by nitric oxide and reactive oxygen species in tobacco Bright-Yellow 2 cells. Plant Physiol **130:** 698–708

Desikan R, Hancock JT, Coffey MJ, Neill SJ (1996) Generation of active oxygen in elicited cells of Arabidopsis thaliana is mediated by a NADPH oxidase-like enzyme. FEBS Lett **382:** 213–217

Dominguez-Solis JR, Gutierrez-Alcala G, Vega JM, Romero LC, Gotor C (2001) The cytosolic O-acetylserine(thiol)lyase gene is regulated by heavy metals and can function in cadmium tolerance. J Biol Chem **276:** 9297–9302

Foissner I, Wendehenne D, Langebartels C, Durner J (2000) In vivo imaging of an elicitor-induced nitric oxide burst in tobacco. Plant J **23:** 817–824

Fojtovà M, Kovařik A (2000) Genotoxic effect of cadmium is associated with apoptotic changes in tobacco cells. Plant Cell Environ **22:** 531–537

Foster MW, Stamler JS (2004) New insights into protein S-nitrosylation: mitochondria as a model system. J Biol Chem **279:** 25891–25897

Gaff DF, Okong'o-Ogola O (1971) The use of the non-permeating pigments for testing the survival of cells. J Exp Bot **22:** 756–758

Garcês H, Durzan D, Pedroso MC (2001) Mechanical stress elicits nitric oxide formation and DNA fragmentation in *Arabidopsis thaliana*. Ann Bot (Lond) **87:** 567–574

Garnier L, Simon-Plas F, Thuleau P, Agnel JP, Blein JP, Ranjeva R, Montillet JL (2006) Cadmium affects tobacco cells by a series of three waves of reactive oxygen species that contribute to cytotoxicity. Plant Cell Environ **29:** 1956–1969

Gould K, Lamotte O, Klinguer A, Pugin A, Wendehenne D (2003) Nitric oxide production by tobacco leaves: a general stress response? Plant Cell Environ **26:** 1851–1862

Heyno E, Klose C, Krieger-Liszkay A (2008) Origin of cadmium-induced reactive oxygen species production: mitochondrial electron transfer versus plasma membrane NADPH oxidase. New Phytol **179:** 687–699

Horemans N, Raeymaekers T, Van Beek K, Nowocin A, Blust R, Broos K,

Cuypers A, Vangronsveld J, Guisez Y (2007) Dehydroascorbate uptake is impaired in the early response of Arabidopsis plant cell cultures to cadmium. J Exp Bot **58:** 4307–4317

Howarth JR, Dominguez-Solis JR, Gutierrez-Alcala G, Wray JL, Romero LC, Gotor C (2003) The serine acetyltransferase gene family in Arabidopsis thaliana and the regulation of its expression by cadmium. Plant Mol Biol **51:** 589–598

Katakai K, Liu J, Nakajima K, Keefer LK, Waalkes MP (2001) Nitric oxide induces metallothionein (MT) gene expression apparently by displacing zinc bound to MT. Toxicol Lett **119:** 103–108

Kovalchuk I, Titov V, Hohn B, Kovalchuk O (2005) Transcriptome profiling reveals similarities and differences in plant responses to cadmium and lead. Mutat Res **570:** 149–161

McCarthy I, Romero-Puertas MC, Palma JM, Sandalio LM, Corpas FJ, Gómez M, del Rio LA (2001) Cadmium induces senescence symptoms in leaf peroxisomes of pea plants. Plant Cell Environ **24:** 1065–1073

Misra RR, Hochadel JF, Smith GT, Cook JC, Waalkes MP, Wink DA (1996) Evidence that nitric oxide enhances cadmium toxicity by displacing the metal from metallothionein. Chem Res Toxicol **9:** 326–332

Murgia I, Tarantino D, Vannini C, Bracale M, Carravieri S, Soave C (2004) Arabidopsis thaliana plants overexpressing thylakoidal ascorbate peroxidase show increased resistance to paraquat-induced photooxidative stress and to nitric oxide-induced cell death. Plant J **38:** 940–953

Nakatsubo N, Kojima H, Kikuchi K, Nagoshi H, Hirata Y, Maeda D, Imai Y, Irimura T, Nagano T (1998) Direct evidence of nitric oxide production from bovine aortic endothelial cells using new fluorescence indicators: diaminofluoresceins. FEBS Lett **427:** 263–266

Neill SJ, Desikan R, Hancock JT (2003) Nitric oxide signalling in plants. New Phytol **159:** 11–35

Noh YS, Amasino RM (1999) Identification of a promoter region responsible for the senescence-specific expression of *SAG12*. Plant Mol Biol **41:** 181–194

Olmos E, Martinez-Solano JR, Piqueras A, Hellin E (2003) Early steps in the oxidative burst induced by cadmium in cultured tobacco cells (BY-2 line). J Exp Bot **54:** 291–301

Ortega-Villasante C, Hernandez LE, Rellan-Alvarez R, Del Campo FF, Carpena-Ruiz RO (2007) Rapid alteration of cellular redox homeostasis upon exposure to cadmium and mercury in alfalfa seedlings. New Phytol **176:** 96–107

Piqueras A, Olmos E, Martinez-Solano JR, Hellin E (1999) Cd-induced oxidative burst in tobacco BY2 cells: time course, subcellular location and antioxidant response. Free Radic Res (Suppl) **31:** S33–S38

Rascio N, Dalla Vecchia F, Ferretti M, Merlo L, Ghisi R (1993) Some effects of cadmium on maize plants. Arch Environ Contam Toxicol **25:** 244–249

Rodriguez-Serrano M, Romero-Puertas MC, Zabalza A, Corpas FJ, Gomez M, Del Rio LA, Sandalio LM (2006) Cadmium effect on oxidative metabolism of pea (Pisum sativum L.) roots: imaging of reactive oxygen species and nitric oxide accumulation in vivo. Plant Cell Environ **29:** 1532–1544

Romero-Puertas MC, Rodríguez-Serrano M, Corpas FJ, Gómez M, del Rio LA, Sandalio LM (2004) Cadmium-induced subcellular accumulation of O^{2-} and H_2O_2 in pea leaves. Plant Cell Environ **27:** 1122–1134

Sandalio LM, Dalurzo HC, Gomez M, Romero-Puertas MC, del Rio LA (2001) Cadmium-induced changes in the growth and oxidative metabolism of pea plants. J Exp Bot **52:** 2115–2126

Sanità di Toppi L, Gabbrielli R (1999) Response to cadmium in higher plants. Environ Exp Bot **41:** 105–130

Schutzendubel A, Polle A (2002) Plant responses to abiotic stresses: heavy metal-induced oxidative stress and protection by mycorrhization. J Exp Bot **53:** 1351–1365

Shigeoka S, Ishikawa T, Tamoi M, Miyagawa Y, Takeda T, Yabuta Y, Yoshimura K (2002) Regulation and function of ascorbate peroxidase isoenzymes. J Exp Bot **53:** 1305–1319

Stamler JS, Toone EJ, Stuart AL, Sucher NJ (1997) (S)NO signals: translocation, regulation, and a consensus motif. Neuron **18:** 691–696

Traas JA, Beven AF, Doonan JH, Cordewener J, Shaw PJ (1992) Cell-cycle dependent changes in labelling of specific phosphoproteins by the monoclonal antibody MPM-2 in plant cells. Plant J **2:** 723–732

Valko M, Morris H, Cronin MT (2005) Metals, toxicity and oxidative stress. Curr Med Chem **12:** 1161–1208

Vanin AF, van Faassen E (2007) Mononitrosyl-iron complexes with dithiocarbamate ligand: physico-chemical properties. *In* E van Faassen, AF Vanin, eds, Radicals for Life: The Various Forms of Nitric Oxide. Elsevier, Amsterdam, pp 383–405

Zottini M, Formentin E, Scattolin M, Carimi F, Lo Schiavo F, Terzi M (2002) Nitric oxide affects plant mitochondrial functionality in vivo. FEBS Lett **515:** 75–78